COBEM 99
XV Congresso Brasileiro de Engenharia Mecânica
15th Brazilian Congress of Mechanical Engineering
22 - 26 de Novembro de 1999 / November 22 - 26, 1999 Águas de Lindóia, São Paulo,

# STRUCTURAL DYNAMIC ANALYSIS OF A TEST STAND FOR LOW POWER PULSED PLASMA THRUSTERS

**Héctor H. Brito**
**Luis A. Lifschitz**
**Rodolfo Duelli**
**Raúl A. Dean**
**Fernando Cappellari**
**Leonardo Molisani**
**Sebastián Maglione**
Group of Computational Mechanics, Mechanics Department, Engineering Faculty.
National University of Rio Cuarto.
Ruta Nacional 36, Km 601, (5800) Río Cuarto, Argentina.Tel – Fax: 054 – 358 – 467 62 46
e – mail : rduelli@ing.unrc.edu.ar

***Abstract.*** *In order to achieve a complete use of the comparative advantages of microsatellites, it is advisable to endow them with autonomous means of orbit control. (Brito & Murgio,1997). Pulsed plasma thrusters are among the most convenient solutions for station keeping, drag compensation, de-orbit and other orbit control alternatives. Ground qualification of this kind of engines requires the impulse bit measurement by means of static firing tests. In this work, a structural and functional analysis of a test stand under development is carried out aiming to assess the performances of pulsed plasma thrusters, mainly by impulse bit determination. A simplified model of the test stand is defined, corresponding eigen modes and frequencies are determined and the dynamic response under pulsed loading is computed, both in the time domain, by using the modal decomposition technique, and in the frequency domain, through spectral analysis techniques. The obtained results allow, at a preliminary level, the adjustment of the test stand design concept so as to optimize the measurement technique.*

***Keywords****: Test stand, Bit impulse, Structural dynamic*

## 1. INTRODUCTION

The aim of this paper is to analyze, from the structural dynamics point of view, a test stand based upon a resonant blade as a sensing device of observable mechanical effects (Fig. 1). The concept is proposed as a low cost alternative and something similar does not seem having previously been reported, according to a literature review (Cubbin ,1996; Meckel *et al.*,1996; Paccani, 1996; Woodruff & Chisel, 1973; Ziemer, *et al*., 1996). Basic performances to be determined by means of static tests are the average thrust and the impulse bit, a measurement range being estimated for the average thrust between 0.1 and 10 mN. The

assumption is made that by mounting the ablative pulsed plasma thruster (APPT) atop the resonant blade and taking advantage of its pulsed working feature will allow the evaluation of these performances, within a prescribed accuracy, where nominal values for the thruster to be tested in this test stand, are shown in Table 1. (Dean *et al*, 1998).

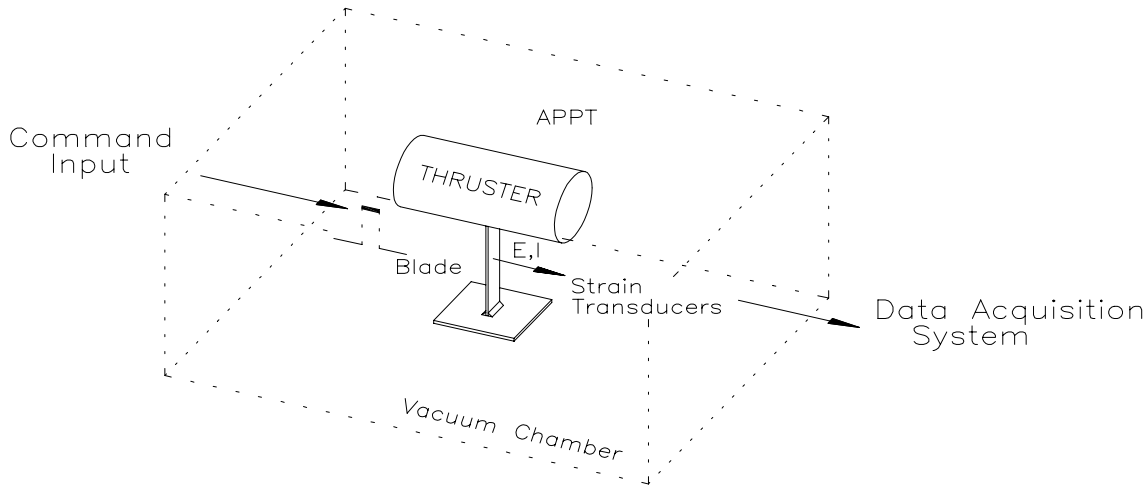


Figure 1: Scheme test stand of resonant blade

Table 1. Characteristics of the thruster to test

| Name | Units | $P^4$ S<br>μ-Sat |
|---|---|---|
| Impulse | [N-s] | 10000 |
| Mass total of the satellite | [kg] | 50 |
| Mass of thruster<br>(propellant + operate) | [kg] | 5 |
| Solid propellant | --- | Teflon |
| Mass of the propellant | [kg] | 2.2 |
| Specific impulse | [s] | 1500 |
| Bit impulse (Ibit) | [μN-s] | 200 |
| Push Average | [mN] | 0.5 |
| Frequency | [Hz] | 2.5 |
| Duration of the bit | [μs] | 1-100 |
| Mass ablationed for Ibit | [μg] | 13.3 |
| External power | [W] | 50 |
| Capacitor | [μF] | 4.7 |

## 2. RESONANT BLADE TEST STAND

### 2.1. General theoretical model

A mathematical model is proposed based on the following assumptions: $H_1$): Firstly, a discrete model of the system is used, i.e., one whose elastic and inertial properties can be described by a finite group of parameters. The structure defined by the flexible blade supporting the APPT, considered as a cylindrical block of M mass and a transverse (with respect to an axis perpendicular to the plan of motion) moment of inertia J, is discretized as a 2 degrees of freedom (d.o.f.) system; one for translational and the other for angular motion. The inertial masses, composed by the APPT and the mechanical interfaces with the resonant blade, is modeled as located in the free end of the resonant blade. $H_2$): A LTI (Linear Time Invariant) system is considered; the motion can then be described by means of a system of second order ordinary differential equations with constant coefficients. $H_3$): It is assumed that the system has a Rayleigh proportional damping.

Accordingly, the system equations of motion, as derived from the Lagrange formulation (Clough & Penzien, 1975) , become:

$$[M]\ \ddot{u}_{(t)} + [C]\ \dot{u}_{(t)} + [\mathrm{K}]\ u_{(t)} = P_{(t)} \qquad (1)$$

$[M]$: generalized mass matrix. $[C]$: matrix of damping coefficients. $[K]$: stiffness matrix of the blade. $P_{(t)}$: generalized force vector acting upon the system. $u_{(t)}$: generalized displacement vector of the system.

where

$$\begin{bmatrix} M & M.r \\ M.r & M.r^2 + J_c \end{bmatrix} \begin{bmatrix} \ddot{x}_{(t)} \\ \ddot{\theta}_{(t)} \end{bmatrix} + \begin{bmatrix} C_{11} & C_{12} \\ C_{21} & C_{22} \end{bmatrix} \begin{bmatrix} \dot{x}_{(t)} \\ \dot{\theta}_{(t)} \end{bmatrix} + \begin{bmatrix} K_{11} & K_{12} \\ K_{21} & K_{22} \end{bmatrix} \begin{bmatrix} x_{(t)} \\ \theta_{(t)} \end{bmatrix} = \begin{bmatrix} F_{(t)} \\ T_{(t)} \end{bmatrix} \qquad (2)$$

The obtained matrices are, in general, non-diagonal.

$F_{(t)}$ , $T_{(t)}$:generalized load vector (force and moment). $x_{(t)}$ , $\theta_{(t)}$: generalized vector of displacement (translation and angular displacement). $M$: mass inertial of thrusters. $r$: radius of thrusters, considered as a cylinder. $J_c$: thrusters mass moment of inertia. $C_{ij}$ : damping matrix coefficient. $K_{ij}$ : stiffness matrix coefficient.

### 2.2. Preliminary sizing of the APPT test stand

The blade was pre-sized so that the displacements and rotations would be small enough to justify the hypothesis which suggests the use of the Lagrangian linear strain tensor without taking into account second order geometrical effects, as those resulting from the weight that manifests as a coupling between the flexural moment and the axial load and lead to the necessity of formulating the mechanical equations of the system in the deformed state. This situation has not been considered in this first approach. An in-house available software was

used to check that the preliminary sizing of the resonant blade conforms to the adopted hypothesis well within the accuracy required by standards and specifications for the test stand qualification. The design criterium for the preliminary sizing is the following: the first natural frequency of the system must coincide with the APPT activation pulsation frequency.

A) Thruster dimensions, considered as a cylinder:
radius $r$ = 0.005 m, length $l$ = 0.20 m, Mass $M$ = 2,5 kg.

B) Resonant blade:
Material: Aluminium, $E$ = 7.1 x $10^{10}$ Pa, $\rho$ = 2.5 x $10^{3}$ kg / $m^3$, $\nu$ = 0.34
Section: rectangular, Thickness: $b$ = 0.003 m, Width: $h$ = 0.03 m, Height: $L$ = 0.150 m.

*Parameter calculations:* A) Thruster: $J$ = 0.0161 kg.m². B) Resonant Blade:

$$K_{11} = \frac{12.E.I}{L^3} = 1.704 \text{ x } 10^4 \text{ N/m} \quad ; \quad K_{12} = -\frac{6.E.I}{L^2} = -1.278 \text{ x } 10^3 \text{ N} = K_{21}$$

$$K_{22} = \frac{4.E.I}{L} = 1.278 \text{ x } 10^2 \text{ N.m} \quad ; \quad I = \frac{b^3.h}{12} = 6.75\text{x}10^{-11} \text{ m}^4$$

$I$ : blade cross section minimal moment of inertia.

Assuming proportional damping of Rayleigh (Humar, 1990). and adopting: $\xi$ = 0.02

$$[C] = \alpha\,[M] + \beta\,[K] \quad ; \quad \alpha = 0.87175 \text{ and } \beta = 0.0001858$$

$\xi_i$ : damping factor associated to the $i$-th mode. $\alpha$ , $\beta$ : proportionality coefficients.

with which the generalized matrices become:

$$[M] = \begin{bmatrix} 2.5 & 0.125 \\ 0.125 & 0.0161 \end{bmatrix} \; ; \; [K] = \begin{bmatrix} 1.704\text{E}04 & -1.278\text{E}03 \\ -1.278\text{E}03 & 1.278\text{E}02 \end{bmatrix} \; ; \; [C] = \begin{bmatrix} 5.3459 & -0.1285 \\ -0.1285 & 0.0378 \end{bmatrix}$$

**2.3. Natural modes and frequencies**

For the case of free vibration the undamped system is described by (Clough & Penzien, 1975):

$$[M]\ddot{\mathbf{u}}_{(t)} + [K]\mathbf{u}_{(t)} = \mathbf{0} \qquad (3)$$

where the natural frequencies of vibration result from the characteristic equation:

$$\det\left[[K] - \lambda\,[M]\right] = 0 \qquad (4)$$

$\lambda_i$ : square of natural frequency associated to the mode $\phi_i$ . $\omega_i$ : natural frequency associated to the mode $\phi_i$ . The eigenvalues are:

$\lambda_1 = \omega_1^2$ = 0.0606E04 ; $\lambda_2 = \omega_2^2$ = 3.6484E04 ; $\omega_1$ = 24.6167 ; $\omega_2$ = 191.0082

and considering that: $f = \frac{\omega}{2.\pi}$ and $T = \frac{2.\pi}{\omega}$

$f$ : undamped natural frequency in hertz. $T$ : undamped natural period in second (s).

we obtain:

$f_1$ = 3.9179 Hz ; $T_1$ = 0.2552 s

$f_2 =$ 30.4 Hz ; $T_2 =$ 0.0329 s

The matrix whose columns are the eigenvectors, i.e., the natural vibration modes of the system, is the modal matrix [$\phi$], given by:

$[\phi]$ : eigenvector matrix. $\phi_i$ : $i$-th eigenvector.

$$[\phi] = \begin{bmatrix} \Phi_1^1 & \Phi_2^1 \\ \Phi_1^2 & \Phi_2^2 \end{bmatrix} \qquad \text{In this case:} \qquad [\phi] = \begin{bmatrix} 0.0869 & -0.0785 \\ 0.9962 & 0.9969 \end{bmatrix}$$

**2.4. State variables equations of the system**

The Equations (1) and (2) can be written in terms of state variables of the system

$$\dot{x} = [A]\, x_{(t)} + [B]\, q_{(t)} \qquad (5)$$

$$y_{(t)} = [F]\, x_{(t)} \qquad (6)$$

being $q_{(t)}$ the input function to the dynamic system, $y_{(t)}$ the output, and $x_{(t)}$ the state vector of the system (Stum & Kirk, 1994).

**2.5. State variables of the system**

The state vector: $[x_{(t)}]^T = [x_{(t)}, \theta_{(t)}, \dot{x}_{(t)}, \dot{\theta}_{(t)}]$

The input function: $[q_{(t)}]^T = [0, 0, F_{(t)}, T_{(t)}]$

The output vector is the same of the state vector

with which the generalized matrices become:

$$[A] = \begin{bmatrix} 0 & 0 & 1 & 0 \\ 0 & 0 & 0 & 1 \\ -17578.1 & 1479.79 & -4.1383 & 0.274991 \\ 215242.1 & -19371.79 & 39.99874 & -4.471639 \end{bmatrix}$$

$$[B] = \begin{bmatrix} 0 & 0 & 0 & 0 \\ 0 & 0 & 0 & 0 \\ 0 & 0 & 0.652631 & -5.052631 \\ 0 & 0 & -5.052631 & 101.052631 \end{bmatrix} \quad ; \quad [F] = \begin{bmatrix} 1 & 0 & 0 & 0 \\ 0 & 1 & 0 & 0 \\ 0 & 0 & 1 & 0 \\ 0 & 0 & 0 & 1 \end{bmatrix}$$

with null initial conditions

## 2.8. Strain sensing model

The impulse bit will basically be obtained in the following way: the amplitude of the displacement in the free end of the blade will be related to the strain measured by a piezoceramic transducer located close to the base of the resonant blade (clamped end).

When it is stressed mechanically by a force, it generates an electric charge. If the electrodes are not short-circuited, a voltage associated with the charge appears.
The mechanical and geometric characteristics of the used sensor are:

$E_s$ = 6.2 x $10^{10}$ Pa, $\rho$ = 7.8 x $10^3$ kg / $m^3$
Length : $L_s$ = 0.0249 m, Width : $h_s$ = 0.006 m, Thickness $b_s$ = 0.0005 m

When a bilaminar element is forced to bend, one layer will be in tension while the other is in compression. Since the two layers are polarized in opposite directions, the opposite stresses in each layer will produce electrical outputs of like polarity. In turn, the strain is determined as related to the electric potential difference between the upper and lower conducting plates of the sensor in its bended configuration. It is assumed that the transducer is perfectly glued to the blade so the strain at the interface has an unique value, i.e. $\varepsilon_l = \varepsilon_s$

Additionally, by assuming a vanishing small transducer (the blade cross section middle line coincides with that of the composed section and will not materially affect the vibrational characteristics of the structure, the transducers are instruments with high natural frequencies), the stress field across the transducer is given by:

$$\sigma(y) = \frac{2E_S\varepsilon}{b} \tag{7}$$

Now, by taking into account the proportionality between electric fields and stresses in piezoelectric materials, represented by a coupling constant g (Piezo Systems, 1993), it follows

$$V = \int g(y)\sigma(y)dy \tag{8}$$

Where:

$$g(y) = \begin{cases} g & for\ \frac{b}{2} + \frac{b_s}{2} < y \le \frac{b}{2} + b_s \\ -g & for\ \frac{b}{2} \le y \le \frac{b}{2} + \frac{b_s}{2} \end{cases}$$

Eq. (7) then becomes

$$V = E_s \frac{b_s^2}{b} \frac{g}{2} \varepsilon \tag{9}$$

Considering that the strain $\varepsilon$ by flexion of the resonant blade may be written as

$$\varepsilon = \frac{M_{base}}{E \ . W} \tag{10}$$

W being the flexural resistant module, given by

$$W = \frac{2I}{b} \tag{11}$$

where b represents the thickness of the resonant blade, and I the cross section minimal moment of inertia. With : $M_{base} = M + F \,.\, L$, where L is the length of the blade. By using Eq. (11) and Eq. (10) one finally obtains:

$$V = E_s \frac{b_s^{\,2} g}{4} \frac{1}{E\,I} M_{base} \tag{12}$$

The transducer was also assumed to be an ideal one, i.e., it does not suffer neither saturation nor any loss in response linearity.

The indicated voltage thus depends on the capacitance of the transducer and indicator circuit. This fact, together with the high impedances normally prevailing in these circuits, determines the approach in the design of piezoelectric transducer and their associated electronic equipment. Owing to the finite insulation resistance, the generated charge gradually leaks away and there is therefore no steady-state response.

At frequencies well below to the transducer natural frequency $f_r$, (the transducers are instruments with high natural frequencies) the equivalent circuit can be simplified as shown in Fig. 2

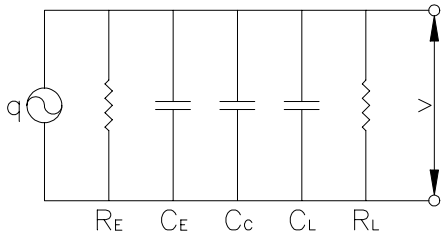


Fig.2 Equivalent circuit of piezoelectric transducers at frequencies below mechanical resonance.

Here q represents the electric charge generated in the transducer, $C_E$ and $R_E$ represent the capacitance and shunt resistance of the transducer element, $C_L$ and $R_L$ are the capacitance and resistance of the load, $C_C$ is the capacitance of the cable between transducer and load, and V represents the observed voltage.

The numerically solved differential equation in the model for the measurement circuit is:

$$\frac{di}{dt} = \frac{1}{R_E C_E}\left(\frac{dq}{dt} - i\right) \tag{13}$$

where for all practical purposes the resistances and the capacitances can be lumped into the total parallel resistance $R_E$ and the total parallel capacitance $C_E$.

## 3. DYNAMIC BEHAVIOR – SIMULATION RESULTS

Once the system was preliminary sized, the general theoretical model allowed its simulation by making use of suitable software, as available in the U.N.R.C. (National University of Rio Cuarto) School of Engineering.

The simulation of the dynamic behavior was made for different input alternatives: (a) a train of rectangular pulses of the same sign with a frequency corresponding to that of the first natural mode, each pulse conforming an impulse bit of 200 μNs; (b) a white noise characterizing a base motion of microseismic origin with a variance of approx. 20E-6 g; (c) the combined action of (a) and (b). Graphs for the cases (a), (b) and (c) of the following quantities are shown in Fig. 4, 5 and 6, respectively: strain transducer output vs. time and strain transducer output vs. frequency. The combinations of 1 N x 200 μseg and 200 N x 1μseg were analyzed, too; the aforementioned Figures correspond to the first of these combinations.

The influence of the impulse bit on the strain transducer output level is observed in Fig. 3 where the results correspond to simulations performed by keeping the same pulse width (200 μseg) while varying the instantaneous constant thrust levels.

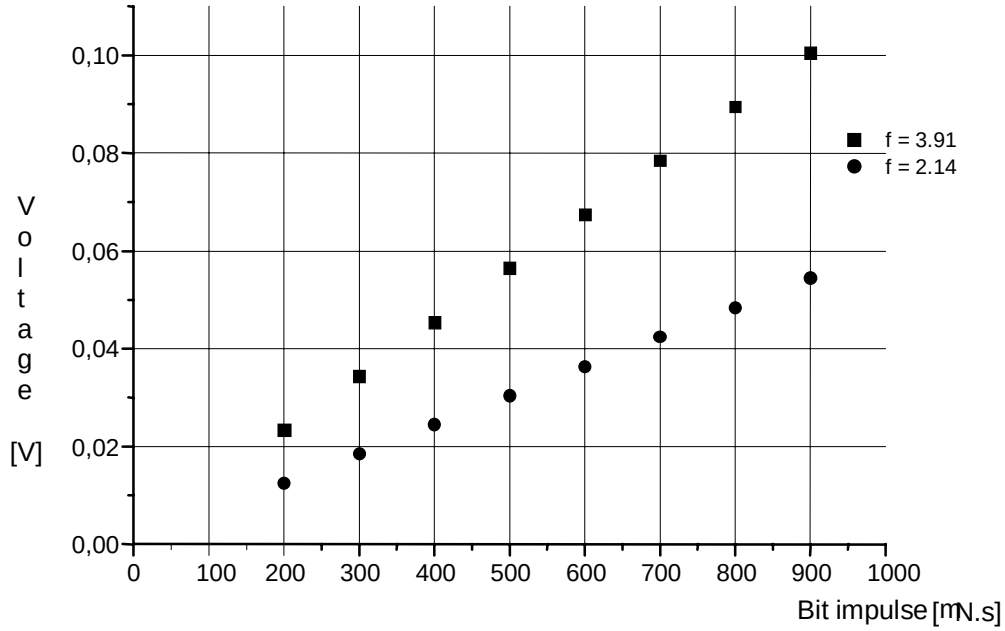


**Fig. 3. Bit Impulse vs Transducer Output**

These simulations made possible to predict the amplitudes of the strain transducer output signal. This signal represents the integrated effect of the APPT thrusting action upon the resonant blade free end, together with the mechanical perturbations of microseismic origin. Neither perturbations of electric origin nor measurement errors were taken into account; it was understood that they do not need to be considered, given the purpose of this preliminary study, mainly aiming to the dynamic behavior analysis of the test stand system.

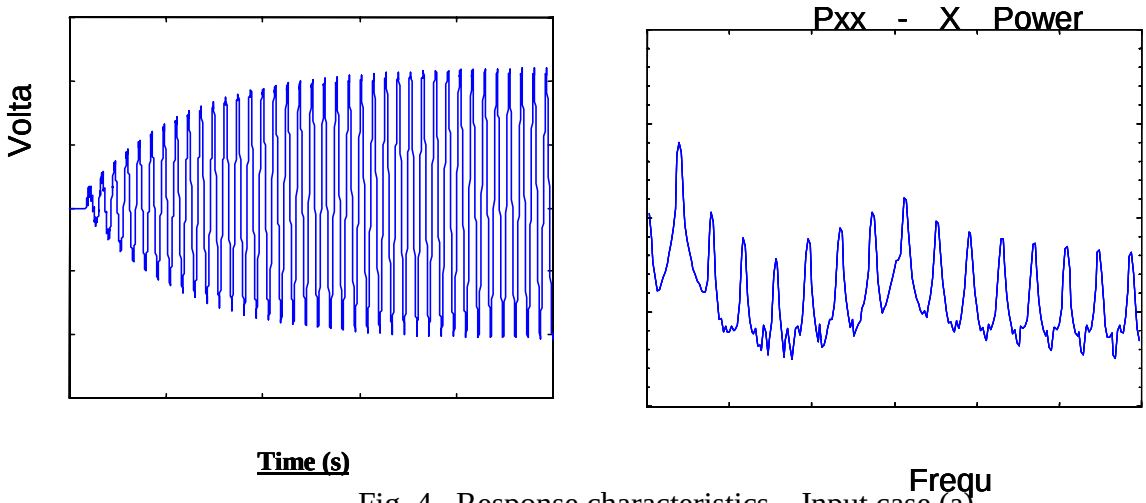


Fig. 4. Response characteristics – Input case (a)

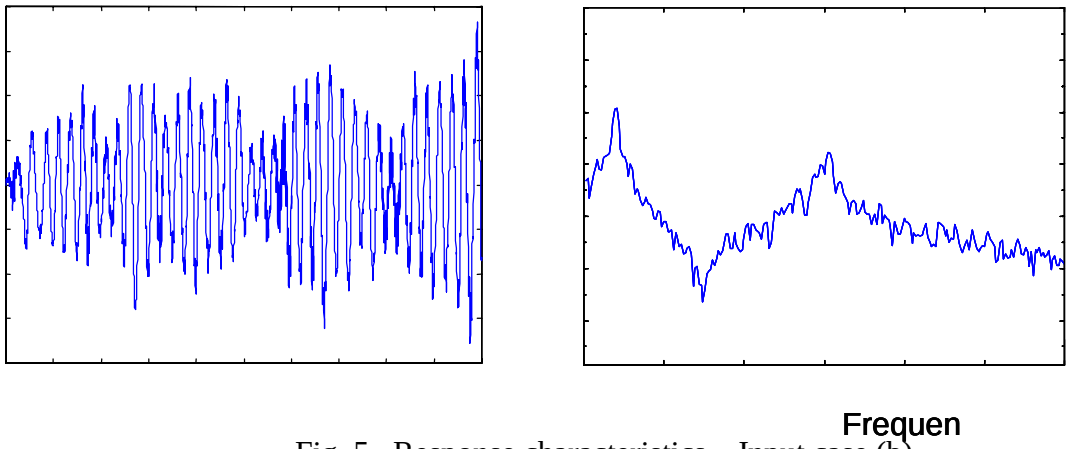


Fig. 5. Response characteristics – Input case (b)

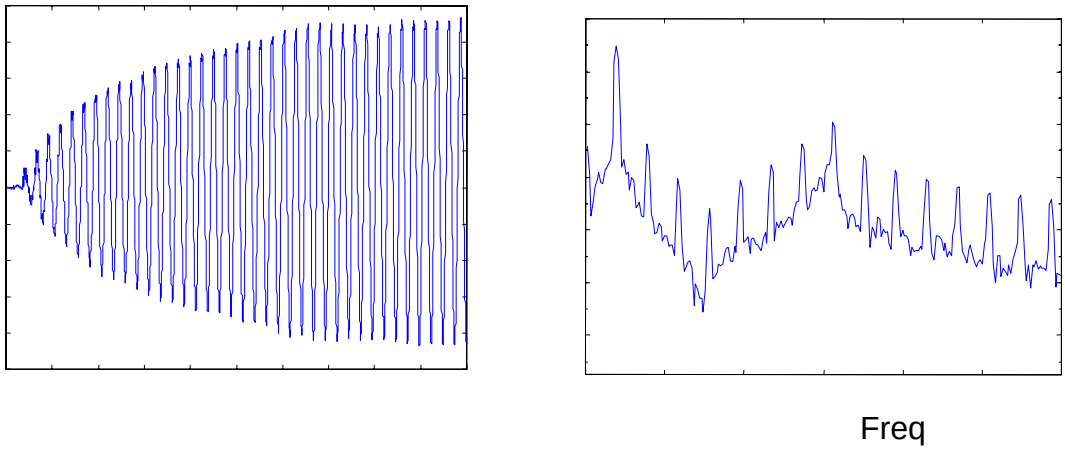


Fig. 6. Response characteristics – Input case (c )

## 4. CONCLUSIONS

Looking at the design concept, the obtained results where the coincidence between the APPT frequency of pulsation with the first natural frequency of the system was sought after, show that the objective of determining the impulse bit by measuring the strain transducer output amplitude, can be reached with S/N (Signal/Noise) ratios which do not jeopardize, in a first approach, the obtaining of current accuracy levels for this kind of test stands (approximately 0.2%).

It should be stressed that the model described throughout this paper is a simplified one aiming at assuring orders of magnitude. A more detailed study should lead to a more rigorous modeling, embracing the system as well as the excitation due to the thrust and the perturbations which should be expected. Indeed, modal testing techniques can give rise to the possibility of improving the model through the adjustment of the theoretical damping factors, mass and stiffness matrices of the system as a function of measured modes and natural frequencies. Further improvements can also be achieved by using numerical filtering techniques that will have the effect of increased S/N ratio, which in turn would allow the time domain identification of the excitation profile.

## REFERENCES


Brito, H. H. & Murgio, L. A., 1997, El proyecto Microsat: primer satélite argentino en órbita, *Ciencia Hoy*, vol. 8, n. 43, pp. 46-49, Buenos Aires, Argentina.

Clough, R.W. & Penzien, J., 1975, Dynamics of Structures, Mc.Graw Hill, U.S.A.

Cubbin, E.A., Ziemer, J. K., Choueiri, E. Y. and Jahn, R. G., 1996, Pulsed thrust measurements using laser interferometry, Paper - American Institute of Aeronautics and Astronautics, Inc. AIAA-96 - 2985.

Dean R., Duelli R., Lifschitz L. and Brito H. H., 1998, Revisión sobre bancos de ensayos para la medición de pequeños impulsos, IV Congreso Anual SOMIM (Sociedad Mexicana de Ingeniería Mecánica), October 22-23, Ciudad de Juarez, Mexico, vol. 1, pp. 288-297.

Humar, J.L., 1990, Dynamics of Structures, Prentice Hall, U.S.A.

Meckel, N. J., Hoskins, W. A. and Cassady, R. J., 1996, Improved pulsed plasma thruster systems for satellite propulsion, AIAA Paper.

Paccani, G., 1996, Solid - propellant quasi-steady MPD thrusters with self - applied magnetic field, AIAA.

Piezo Systems, Inc. , 1993, Product catalog, U.S.A.

Stum, R. D. & Kirk, D. E., 1994, Contemporary Linear Systems. Using MATLAB, PWS Publishing Company, Boston, U.S.A.

Woodruff, J. R. & Chisel, D. M., 1973, Test stand for precise measurement of impulse an thrust vector of small attitude control jets, NASA Technical Note D-7402, August, Washington, D.C., pp. 01-36.

Ziemer, J.K., Cubbin, E.A. and Choueiri, E.Y., 1996, Pulsed plasma propulsion for a small satelite: mission COMPASS $P^3$OINT, AIAA-96-3292.